Towards entangled photon pair generation from SiC-based microring resonator

Anouar Rahmouni*[a], Lijun Ma[1], Lutong Cai[2], Xiao Tang[1], Thomas Gerrits[1], Qing Li[2], Oliver Slattery[1]

[1] *National Institute of Standards and Technology, 100 Bureau Dr, Gaithersburg, MD 20899, USA*
[2]*Department of Electrical and Computer Engineering, Carnegie Mellon University, Pittsburgh, PA 15213, USA*

ABSTRACT

Entangled photon sources are fundamental building blocks for quantum communication and quantum networks. Recently, silicon carbide has emerged as a promising material for integrated quantum devices since it is CMOS-compatible with favorable mechanical, electrical and photonic properties. In this work, we report on our progress toward entangled photon pair generation at the telecom wavelength (1550 nm) via implementing spontaneous four-wave mixing in a compact silicon carbide microring resonator. We will present the design principle, experimental set-up, and results.

1. INTRODUCTION

Entangled photon sources are essential components in quantum communication and networking systems [1,2,3]. So far, entangled photon pair sources and quantum interfaces are predominantly based on bulk materials or weakly confined waveguides in periodically poled nonlinear optical crystals such as lithium niobate (PPLN) [4,5] or potassium titanyl phosphate (PPKTP) [6]. However, neither PPLN nor PPKTP can be directly integrated on semiconductor wafers. On the other hand, while many efforts have been made to optimize quantum-dot-based quantum sources in hybrid nanophotonic structures [7], their application is typically limited by the need for cryogenic operation [8].

Recently, silicon carbide (SiC) emerged as a promising material for both classical and quantum applications [9, 10], as it is compatible with metal-oxide semiconductor (CMOS) foundry processes and has many favorable mechanical, electrical and photonic properties [11]. For example, SiC is transparent from approximately 400 nm to 5000 nm; possesses simultaneous second- and third-order optical nonlinear coefficients; and has large thermal conductivity which is helpful for heat dissipation [12,13]. In addition, SiC hosts various color centers ranging from the visible to the NIR and in the telecom-band spectral region, which can be exploited for use as single-photon sources or quantum memories [14, 15]. Finally, high-quality SiC wafers up to six inches are already commercially available, with n- and p-type doping methods well established for CMOS integrated-circuits fabrication processing [16].

To take full advantage of the unique material properties offered by SiC, a thin-film SiC-on-insulator integrated platform has been successfully demonstrated [17], which can potentially reduce the device's SWaP (size, weight, and power) while increasing functionalities at the chip level [18]. Efforts on nanofabrication have dramatically reduced the propagation loss on chip [19], making SiC a competitive choice even when compared to more mature integrated photonics platforms such as silicon-on-insulator [20] or lithium niobate-on-insulator [21]. In fact, optical quality factors (Qs) in the 5 to 8 million range [22], indicating a propagation loss well below 1 dB/cm have been achieved. Relevant to quantum applications, single-photon detectors based on superconducting nanowires have also been integrated on the SiC platform [23].

Despite the research progress made on the SiC color centers over the past few years, to the best of our knowledge, entangled photon pair generation at the telecom wavelength (C band) is yet to be demonstrated. Here, we report the first measurement of correlated photon pair generation by implementing efficient spontaneous four-wave mixing (SFWM) in a compact SiC microring resonator, which forms the basis for an entangled photon pair source that can be used to encode quantum information on multiple degrees of freedom such as time bin [24] and polarization [25].

* anouar.rahmouni@nist.gov ; https://www.nist.gov

2. DEVICE FABRICATION

In this work, a compact 36-μm-radius SiC microring resonator is employed for the photon pair generation. The device fabrication starts with depositing 2 μm Plasma-enhanced chemical vapor deposition (PECVD) oxide on a vanadium-doped 4H-SiC (II-VI inc) wafer, which is bonded to a silicon carrier and subsequently polished to a thickness of 500 nm. On-chip waveguides and resonators are then patterned using e-beam lithography and transferred to the SiC layer with CHF_3/O_2 based dry etching. Our optimized nanofabrication has resulted in optical *Q*s above 1 million for 36 μm-radius SiC microring resonators (see Fig. 1). In addition, dispersion engineering can be carried out by varying the ring waveguide width, covering the anomalous, zero, and normal dispersions all on the same chip. Thanks to the strong Kerr nonlinearity offered by SiC, such devices have already been used to demonstrate broadband microcombs [12]. Here, we will focus on the quantum version of the comb generation (i.e., SFWM) by reducing the optical power to far below the threshold. To couple light to and from the chip, grating couplers are employed which show a coupling loss on the order of 5 to 8 dB. Linear characterization confirms that for ring widths around 1.8 μm, the dispersion of the fundamental TE (transverse-electric) mode is small enough to allow efficient photon pair generation near the pump wavelength.

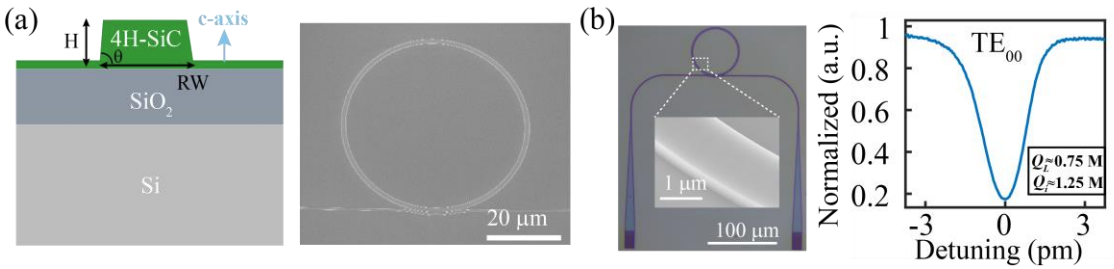

Figure 1: (a) Left: schematic of the 4H-silicon-carbide-on-insulator platform that consists of 500 nm vanadium-doped SiC on top of a 2-μm-thick PECVD dioxide layer. Right: Scanning electron micrograph of a 36 μm-radius SiC microring. (b) Left: Grating couplers are employed for the coupling of light, with a typical insertion loss around 5 to 8 dB per grating. Right: Representative resonance for the fundamental TE mode (TE_{00}), showing an intrinsic quality Q_i of 1.25 million and a loaded quality Q_l of 0.75 million.

3. EXPERIMENTAL CONFIGURATION

Our experimental schematic for the photon pair generation in the C band is illustrated in Fig. 2. The pump light, formed by a tunable continuous-wave (CW) telecom pump laser going through an Erbium-Doped Fiber Amplifier (EDFA), first goes through a narrow bandpass filter consisting of seven cascaded 100 GHz dense wavelength division multiplexers (DWDMs) for selecting the laser line (1550.12 nm ± 0.11 nm) while rejecting light out of band by up to 150 dB. It is then coupled to the SiC chip through a grating-based coupler with an approximate 6 dB coupling loss. The light coming out of the SiC chip is collected using another grating before being sent to a pump-notch filter consisting of four fiber Bragg grating (FBG) filters and five 100 GHz DWDMs. We then employ a 32-channel DWDM with a 100 GHz channel separation to filter the signal and idlers photons into the ITU-29 (1554.13 nm) and ITU-39 (1546.12 nm) channels, respectively. For the photon detection, we use two superconducting nanowire single-photon detectors (SNSPDs) with a detection efficiency > 90 % at 1550 nm and a dark count rate <500 counts/s. The coincidence measurement is carried out by sending the output from the detectors to a time tagger with a time-bin size of 160 ps.

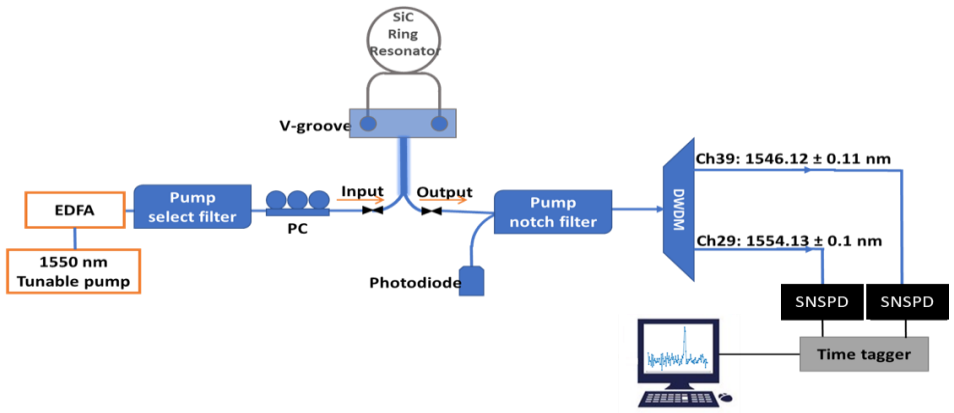

Figure 2: Experimental setup for the photon pair generation in SiC: The pump light, formed by a tunable laser going through an EDFA, first goes through a narrow bandpass filter for selecting the laser line (1550.12 nm ± 0.11 nm) while rejecting light out of band by up to 150 dB. A fiber polarization controller (PC) is then used to optimize coupling efficiency to the SiC chip through a grating-based coupler with an approximate 6 dB coupling loss. The light coming out of the SiC chip is collected using another grating before being sent to a pump-notch filter. An ITU compatible DWDM is employed subsequently to select the signal and idler photons. We use two superconducting nanowire single-photon detectors (SNSPDs) and a time tagger for the coincidence measurement.

The use of DWDM filters necessitates the alignment of the microring resonance to the select ITU wavelength grids. For this purpose, we mount the SiC chip on a temperature-controlled stage, whose temperature can be varied from 27 °C to 100 °C. The resonance wavelength shows an approximate 10 pm/°C dependence. In addition, to compensate for the optical losses from all the optical filters, we use a relatively large pump power (on-chip power on the order of 10 mW), which leads to thermal bistability in the swept-wavelength transmission measurement due to partial optical absorption (Fig. 3). In the experiment, we carefully adjust the stage temperature while also accounting for an absorption-induced wavelength shift such that the transmission dip (i.e., the bottom of the thermal triangle) coincides with the desired ITU grid.

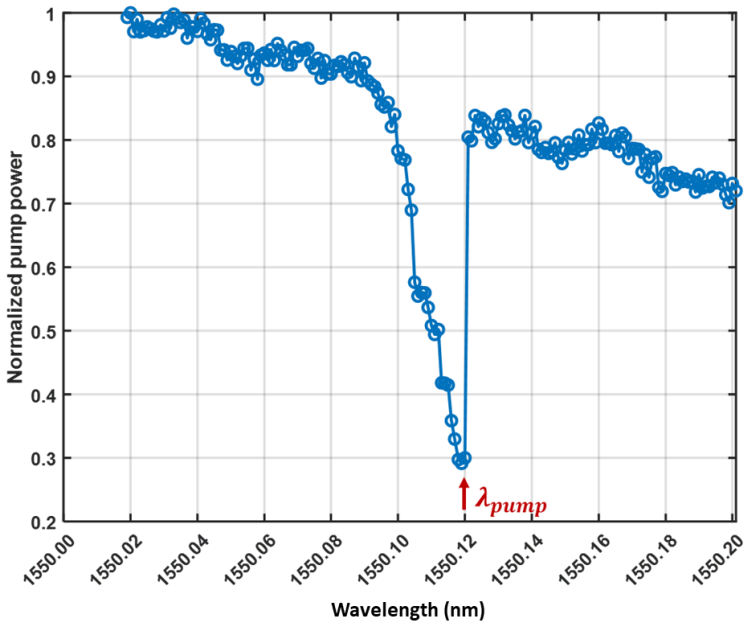

Figure 3: Swept-wavelength transmission measurement of a 36-μm-radius SiC microring resonator with an on-chip power around 6.8 mW, where thermal bistability is observed. The resonance dip is tuned to the ITU-34 grid (1550.12 nm) by varying the stage temperature (in this case set at 85 °C).

4. EXPERIMENTAL RESULTS

We detected photon flux above the noise floor in the signal/idler channel with mW-level pump power. For example, when the on-chip power is around 6.8 mW, the SNSPD for the signal registered 0.3M counts/s, indicating aflux of >10M photons/s on the chip after accounting for all the insertion losses (approximately 6 dB from grating and 10 dB from off-chip filters) and detector efficiency. Using the experimental setup described in Fig. 2, coincidence counts between the select signal and idler photons (see Fig. 2) were also successfully detected, with a measured rate around 100 counts/s for the on-chip power of 6.8 mW. After subtracting the noise and normalizing the coincidence counts, we estimate the FWHM of the coincidence spectrum to be around 2 ns (Fig. 4), which is consistent with the million-level *Q* of the optical resonances. Although a SFWM-based quantum comb in 4H-SiC has been demonstrated, the prior work is focused on the study of their second-order correlation in the context of the microcomb soliton state [22]. To the best of our knowledge, this is the first time that the coincidence between the energy-correlated signal-idler photon pair has ever been reported in any SiC platforms. Our result also indicates that the SiC-oxide interface is not as noisy as suggested by earlier works [26], and we note that no annealing or other treatment has been performed for our SiC microrings.

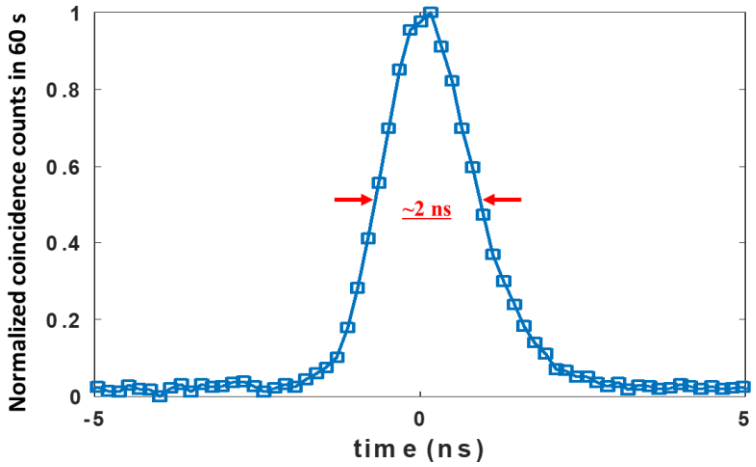

Figure 4: Normalized coincidence spectrum for the select signal/idler pair shown in Fig. 2. The FWHM of the coincidence counts is estimated to be around 2 ns.

Next, we vary the pump power to perform a more systematic characterization of the coincidence rate and the noise involved in the process. Figure 5(a) shows the raw coincidence counts for on-chip pump power varied from 6 mW to 12 mW, with the corresponding coincidence-to-accidental (CAR) ratio shown in Fig. 5(b). Currently, our CAR is estimated to be in the 3 to 4 range, which is partly limited by the Raman noise generated in the significant number of fiber-based filters (>10) used in our experimental setup (see Fig. 2). In fact, by bypassing the SiC chip, we can measure a similar level of noise on our detectors, suggesting that most of the noise comes from the light propagating in the fibers. In the future, we plan to include on-chip filters on the SiC chip to reduce the overall fiber length as well as the insertion loss, and hence improve the CAR to the level suitable for practical quantum applications.

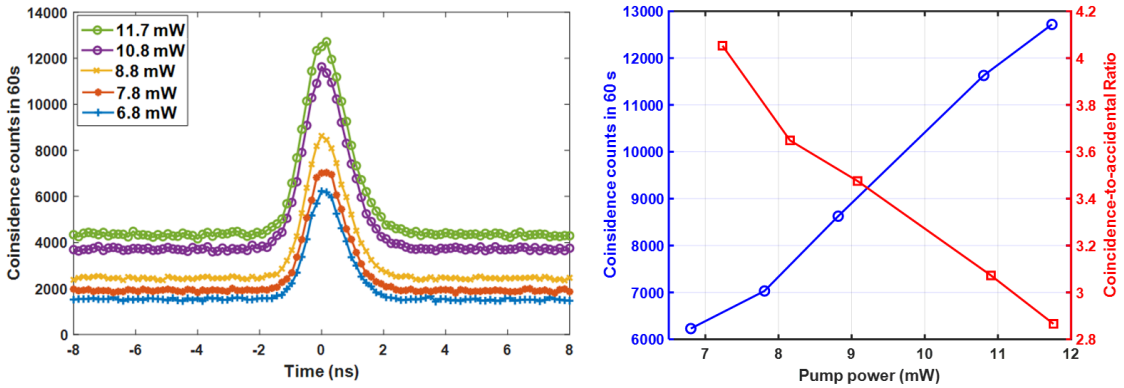

Figure 5: (a) Raw coincidence counts in 60 s and (b) coincidence-to-accidental ratio (CAR) for varied pump powers from 6.8 mW to 11.7 mW on chip.

5. CONCLUSION

To conclude, we have experimentally demonstrated photon pair generation in the telecom wavelength band (1550 nm) in a 4H-SiCOI platform. To our knowledge, this is the first time that coincidences between the energy-correlated signal-idler photon pair has been reported in any SiC platform. By pumping a high-*Q* SiC microring resonator, signal/idler photon flux on the order of a million photons/s and coincidence rate >12000 counts/60s has been measured for an on-chip power on the order of 10 mW. So far, the coincidence-to-accidental ratio is limited by the spontaneous Raman scattering from the significant number of fiber-based filters used in this work. In the future, we plan to use on-chip filters to reduce the Raman noise and hence improve the CAR value.

6. DISCLAIMER

Certain commercial equipment, instruments, or materials are identified in this paper to foster understanding. Such identification does not imply recommendation or endorsement by the National Institute of Standards and Technology, nor does it imply that the materials or equipment identified are necessarily the best available for the purpose.

7. REFERENCES

[1]: Knill, E., Laflamme, R., & Milburn, G. J. (2001). A scheme for efficient quantum computation with linear optics. Nature, 409(6816), 46-52.

[2]: Yuan, Z. S., Bao, X. H., Lu, C. Y., Zhang, J., Peng, C. Z., & Pan, J. W. (2010). Entangled photons and quantum communication. Physics Reports, 497(1), 1-40.

[3]: O'brien, J. L., Furusawa, A., & Vučković, J. (2009). Photonic quantum technologies. Nature Photonics, 3(12), 687-695.

[4]: Alibart, O., D'Auria, V., De Micheli, M., Doutre, F., Kaiser, F., Labonté, L., ... & Tanzilli, S. (2016). Quantum photonics at telecom wavelengths based on lithium niobate waveguides. Journal of Optics, 18(10), 104001.

[5]: Alibart, O., D'Auria, V., De Micheli, M., Doutre, F., Kaiser, F., Labonté, L., ... & Tanzilli, S. (2016). Quantum photonics at telecom wavelengths based on lithium niobate waveguides. Journal of Optics, 18(10), 104001.

[6]: Usmani, I., Clausen, C., Bussières, F., Sangouard, N., Afzelius, M., & Gisin, N. (2012). Heralded quantum entanglement between two crystals. Nature Photonics, 6(4), 234-237.

[7]: Kim, J. H., Aghaeimeibodi, S., Richardson, C. J., Leavitt, R. P., Englund, D., & Waks, E. (2017). Hybrid integration of solid-state quantum emitters on a silicon photonic chip. Nano letters, 17(12), 7394-7400.

[8]: Arakawa, Y., & Holmes, M. J. (2020). Progress in quantum-dot single photon sources for quantum information technologies: A broad spectrum overview. Applied Physics Reviews, 7(2), 021309.

[9]: Lohrmann, A., Johnson, B. C., McCallum, J. C., & Castelletto, S. (2017). A review on single photon sources in silicon carbide. Reports on Progress in Physics, 80(3), 034502.

[10]: Xu, M., Girish, Y. R., Rakesh, K. P., Wu, P., Manukumar, H. M., Byrappa, S. M., & Byrappa, K. (2021). Recent advances and challenges in silicon carbide (SiC) ceramic nanoarchitectures and their applications. Materials Today Communications, 28, 102533.

[11]: Castelletto, S., Peruzzo, A., Bonato, C., Johnson, B. C., Radulaski, M., Ou, H., ... & Wrachtrup, J. (2022). Silicon Carbide Photonics Bridging Quantum Technology. ACS Photonics, 9(5), 1434-1457.

[12]: L. Cai, J. Li, R. Wang, and Q. Li, "Octave-spanning microcomb generation in 4H-silicon-carbide-on-insulator photonics platform," Photon. Res., PRJ 10, 870–876 (2022).

[13]: Naftaly, M., Molloy, J. F., Magnusson, B., Andreev, Y. M., & Lanskii, G. V. (2016). Silicon carbide—a high-transparency nonlinear material for THz applications. Optics express, 24(3), 2590-2595.

[14]: Castelletto, S., & Boretti, A. (2020). Silicon carbide color centers for quantum applications. Journal of Physics: Photonics, 2(2), 022001.

[15]: Bourassa, A., Anderson, C. P., Miao, K. C., Onizhuk, M., Ma, H., Crook, A. L., ... & Awschalom, D. D. (2020). Entanglement and control of single nuclear spins in isotopically engineered silicon carbide. Nature Materials, 19(12), 1319-1325.

[16]: Castelletto, S. (2021). Silicon carbide single-photon sources: challenges and prospects. Materials for Quantum Technology, 1(2), 023001.

[17]: Lukin, D. M., Guidry, M. A., & Vučković, J. (2020). Integrated quantum photonics with silicon carbide: challenges and prospects. PRX Quantum, 1(2), 020102.

[18]: Kaplar, R. J., Neely, J. C., Huber, D. L., & Rashkin, L. J. (2017). Generation-After-Next Power Electronics: Ultrawide-bandgap devices, high-temperature packaging, and magnetic nanocomposite materials. IEEE Power Electronics Magazine, 4(1), 36-42.

[19]: Guidry, M. A., Yang, K. Y., Lukin, D. M., Markosyan, A., Yang, J., Fejer, M. M., & Vučković, J. (2020). Optical parametric oscillation in silicon carbide nanophotonics. Optica, 7(9), 1139-1142.

[20]: Pavesi, L. (2003). Will silicon be the photonic material of the third millenium? Journal of Physics: Condensed Matter, 15(26), R1169.

[21]: Poberaj, G., Hu, H., Sohler, W., & Guenter, P. (2012). Lithium niobate on insulator (LNOI) for micro-photonic devices. Laser & photonics reviews, 6(4), 488-503.

[22]: Guidry, M. A., Lukin, D. M., Yang, K. Y., Trivedi, R., & Vučković, J. (2022). Quantum optics of soliton microcombs. Nature Photonics, 16(1), 52-58.

[23]: Martini, F., Gaggero, A., Mattioli, F., & Leoni, R. (2019). Single photon detection with superconducting nanowires on crystalline silicon carbide. Optics Express, 27(21), 29669-29675.

[24]: Brendel, J., Gisin, N., Tittel, W., & Zbinden, H. (1999). Pulsed energy-time entangled twin-photon source for quantum communication. Physical Review Letters, 82(12), 2594.

[25] Peters, N. A., Barreiro, J. T., Goggin, M. E., Wei, T. C., & Kwiat, P. G. (2005). Remote state preparation: arbitrary remote control of photon polarization. Physical review letters, 94(15), 150502.

[26]: Lukin, D. M., Dory, C., Guidry, M. A., Yang, K. Y., Mishra, S. D., Trivedi, R., ... & Vučković, J. (2020). 4H-silicon-carbide-on-insulator for integrated quantum and nonlinear photonics. Nature Photonics, 14(5), 330-334.